Supplementary information

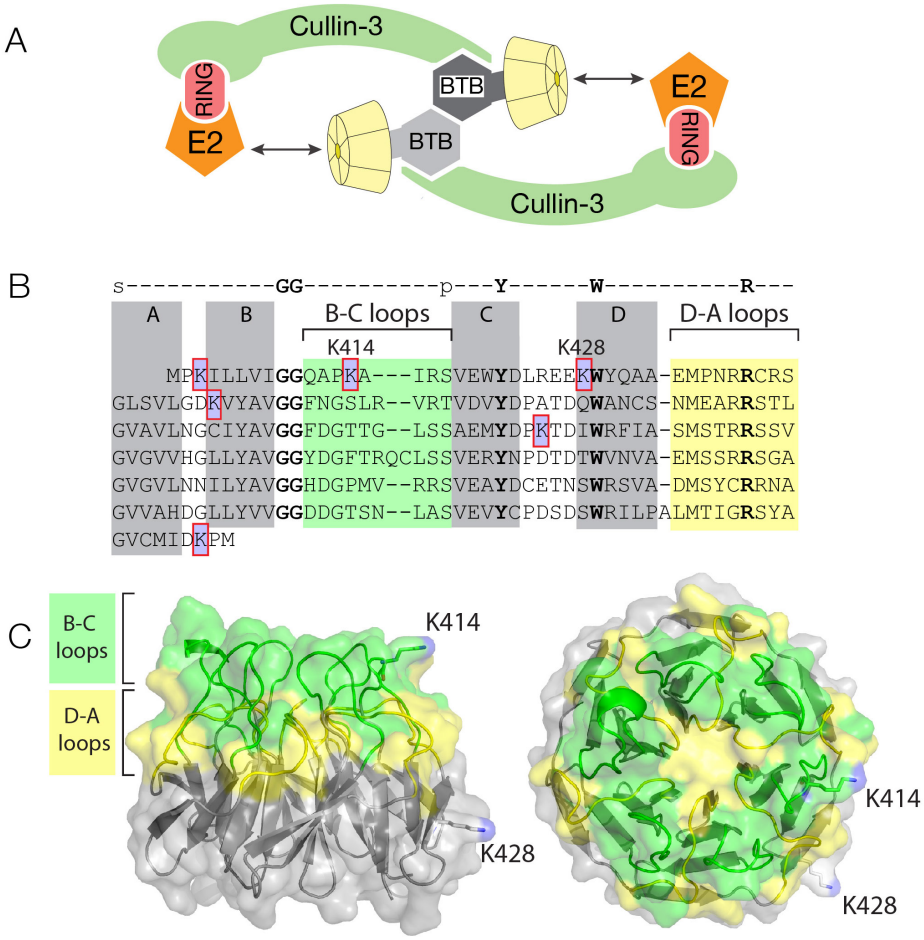

Figure S1. Lysine residue positions in Kelch KREP domain. (A) 2D cartoon of hypothetical CRL3^{Kelch} structure based on structural modeling in (Stogios et al., 2005). The "top", substrate binding surface of each KREP domain is oriented toward the E2 ubiquitin conjugating enzyme. SRS autoubiquitylation can be inhibited when excess substrate is present (Deshaies, 1999), consistent with SRS autoubiquitylation occurring across the cleft between the SRS substrate binding domain and the E2 enzyme (double arrow). (B) Sequence of Kelch KREP domain. The six lysine residues are indicated. The four β-strands that make up each blade of the β-propeller structure are highlighted in gray and labeled A - D. Sequence loops between the B-C and D-A strands are highlighted in in green and yellow, respectively, and correspond to the green and yellow structural elements in C. (C) Homology model of Drosophila Kelch created using the Phyre2 homology modeling server (http://www.sbg.bio.ic.ac.uk/~phyre2/; Kelley and Sternberg, 2009) based on the structure of the human Kelch ortholog KLHL2/Mayven (PDB: 2XN4; Canning et al., 2013). Two lysine residues, K414 and K428, are surface-exposed, and K414 is located in a B-C loop extending from the 'top' surface of the Kelch β-propeller, presumably oriented toward the E2 enzyme in the assembled CRL.

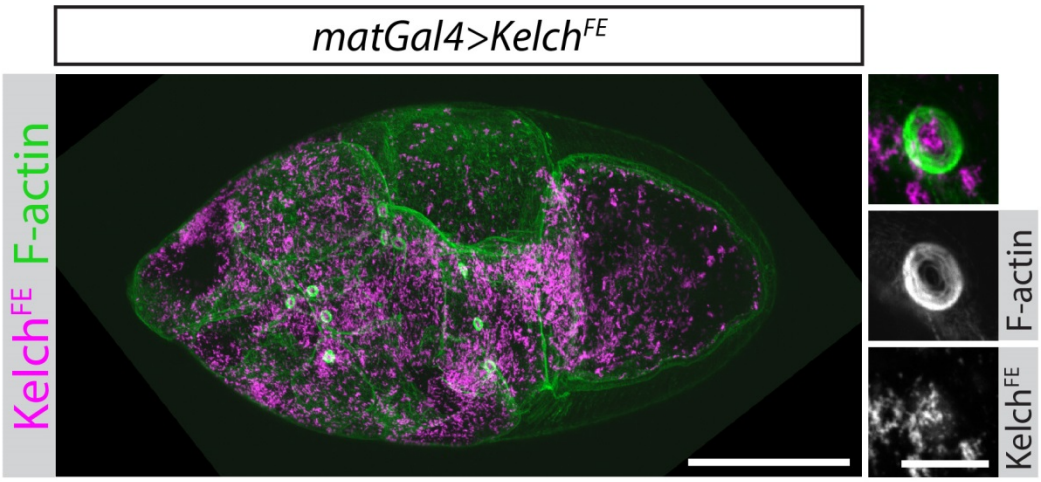

Figure S2. Overexpression of Kelch^{FE} results in a dominant-negative *kelch*-like phenotype. (A) Kelch^{FE} was expressed in wild-type germ cells using the strong *matGal4* driver. The stage 10 egg chamber shown has a small oocyte, indicating that nurse cell-to-oocyte transport is compromised (compare to wild-type and *kelch* mutant egg chambers in Figure 3 A and B). Ring canals are occluded with disorganized F-actin (insets). Scale bars: 50 μm for egg chamber image, 10 μm for ring canal inset.

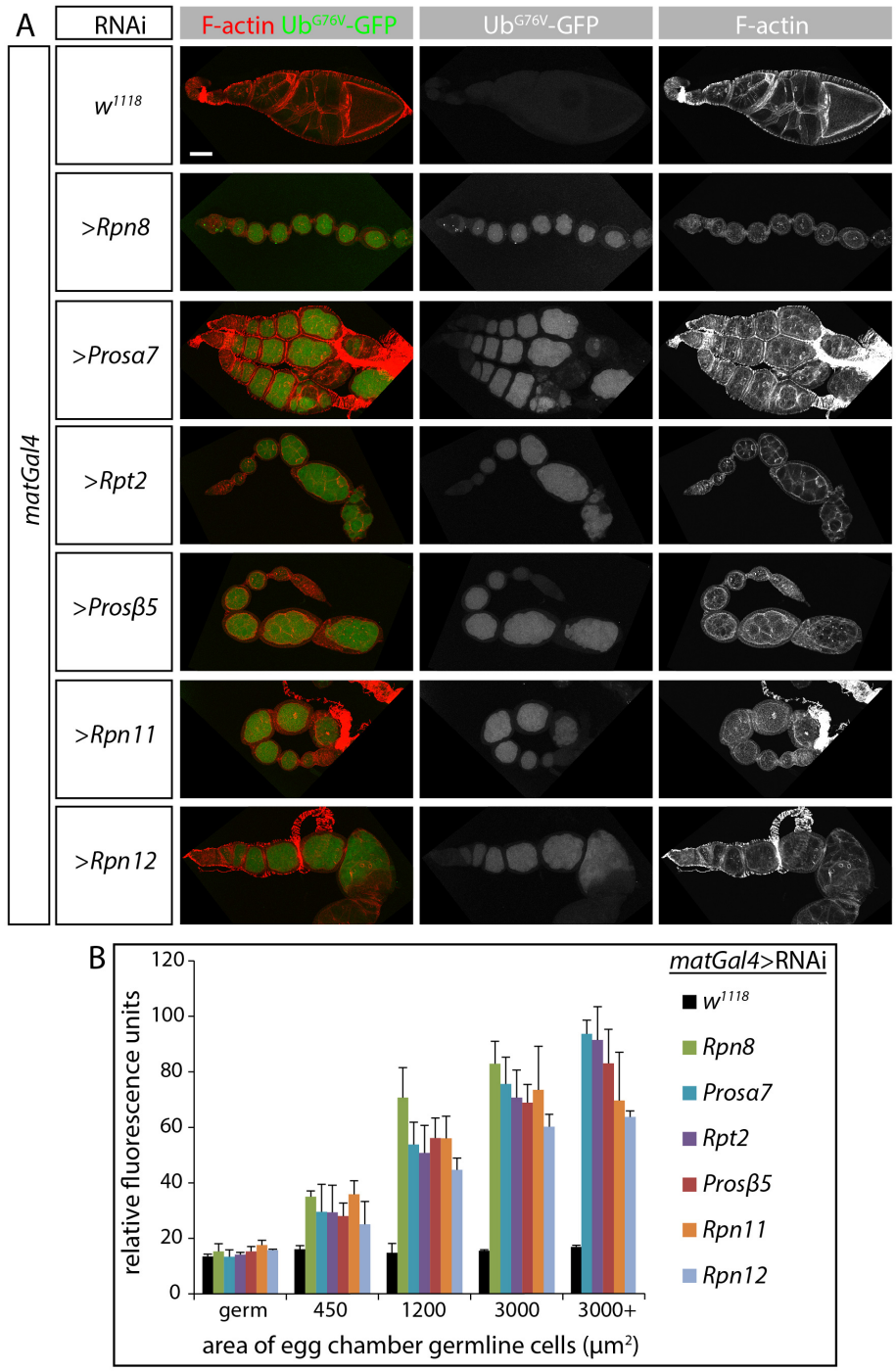

Figure S3. Multiple RNAi lines are effective at inhibiting the proteasome as evidenced by Ub^{G76V}-GFP accumulation. (A) Ub^{G76V}-GFP proteasome activity reporter accumulates upon proteasome inhibition with various RNAi lines targeting proteasome subunits. (B) Quantification of Ub^{G76V}-GFP reporter for each RNAi line. Note that *matGal4>Rpn8 RNAi* egg chambers have the highest extent of Ub^{G76V}-GFP reporter protein and the most severe growth arrest (no egg chambers in '3000+ μm^2' area grouping). Scale bar: (A) 50 μm

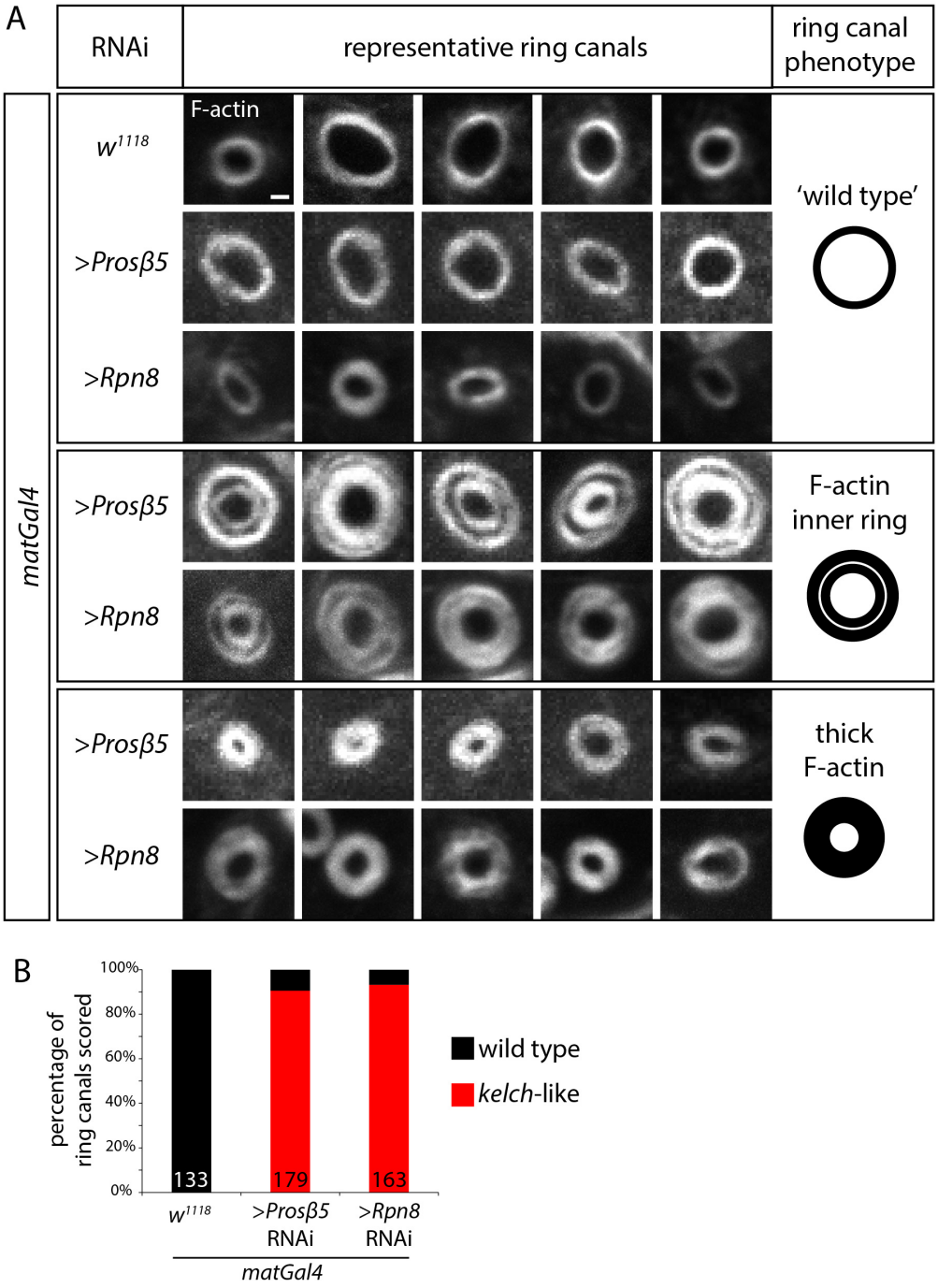

Figure S4. Proteasome inhibition by RNAi leads to high penetrance of *kelch*-like ring canals. (A) Proteasome inhibition by RNAi (targeting Prosβ5 or Rpn8 proteasome subunits) results in different classes of ring canal phenotypes: (top) morphologically normal ("wild type") ring canals, (middle) ring canals with a prevalent inner ring of F-actin, (bottom) ring canals with a thick, *kelch*-like F-actin ring. (B) Quantification of penetrance of *kelch*-like ring canals. Ring canals that displayed an aberrant F-actin ring or had abnormally thicker F-actin rings were deemed *kelch*-like. Sample size is indicated at the base of each bar. Scale bar: (A) 1 μm.

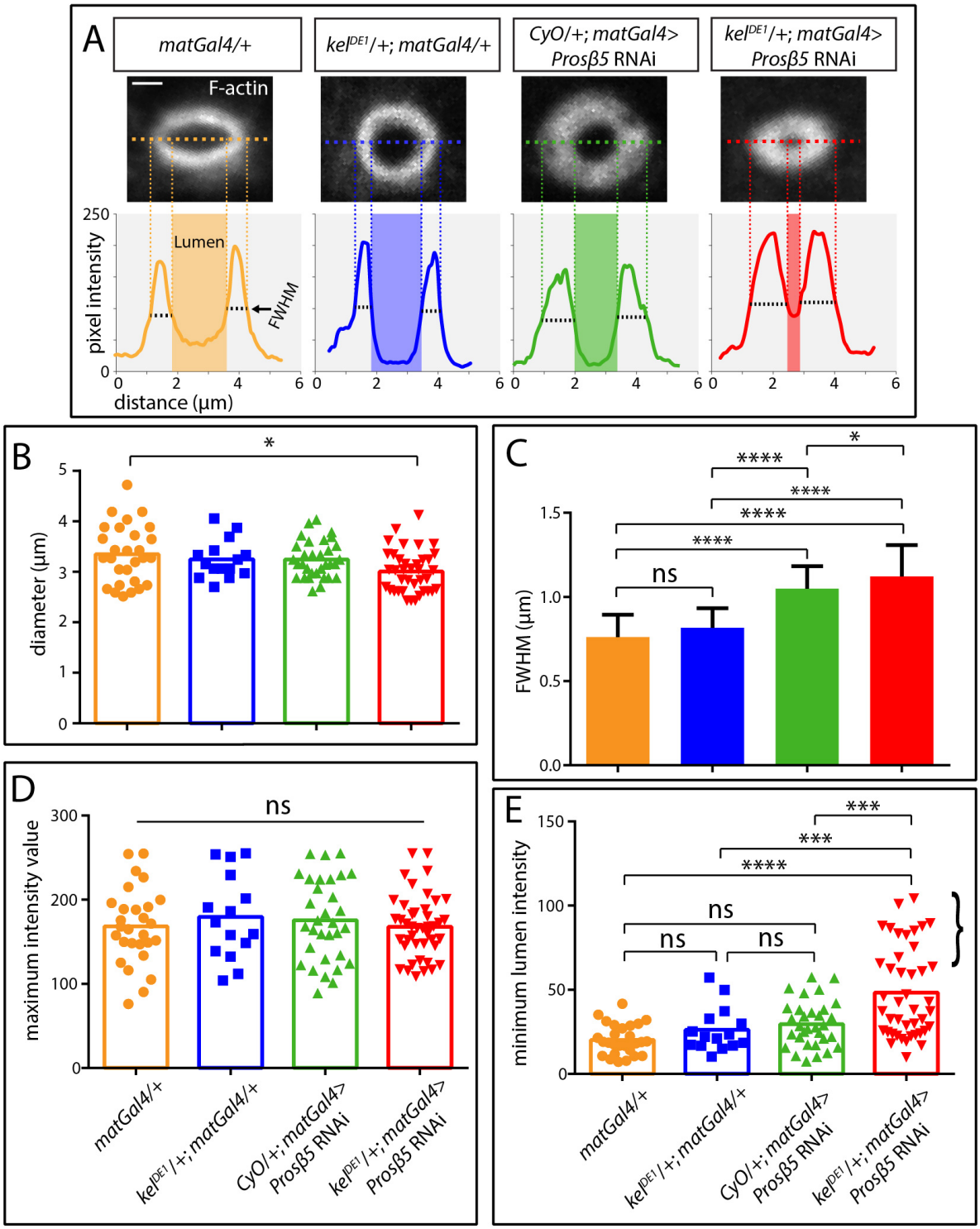
A
matGal4/+
kelDE1/+; matGal4/+
CyO/+; matGal4> Prosβ5 RNAi
kelDE1/+; matGal4> Prosβ5 RNAi
F-actin
Lumen
FWHM
pixel intensity
distance (μm)
B
diameter (μm)
C
FWHM (μm)
ns
D
maximum intensity value
matGal4/+
kelDE1/+; matGal4/+
CyO/+; matGal4> Prosβ5 RNAi
kelDE1/+; matGal4> Prosβ5 RNAi
E
minimum lumen intensity

Figure S5. Loss of one copy of *kelch* dominantly enhances the *kelch*-like phenotype with proteasome inhibition. (A) Quantification of ring canal F-actin intensity plot allows for accurate measurement of key ring canal parameters. Using FIJI, intensity plots were acquired across the span of ring canals. Horizontal dotted colored line across each ring canal corresponds to plotted line below of F-actin intensity values. The full width at half maximum (FWHM) (black dotted lines) accurately corresponds to the boundaries of the ring canal F-actin. The ring canal lumen was calculated as the distance spanned between the two inner half maximum points (lumen represented by shaded box). (B) Quantification and distribution of ring canal diameters measured for analysis. The ring canal diameter is the distance spanned by the two outer half maximum points. Colored points represent all measurements and bars represent mean diameter. Ring canals analyzed were of similar sizes. (C) Quantification of FWHM - a representation of ring canal F-actin thickness. Filled-in bars represent FWHM mean and error bars show standard deviation. (D) Quantification and distribution of maximum intensity values measured. The distributions of maximum F-actin intensity values across analyzed ring canals were similar, indicating that staining and imaging conditions were comparable across samples. (E) Quantification of minimum intensity value of F-actin within the lumen of each ring canal. Colored points represent all measurements and bars represent the mean lumen intensity value. Note the appearance of points with high minimum lumen intensity values with loss of one copy of *kelch* in addition to proteasome inhibition. This indicates dominant enhancement of the *kelch*-like phenotype, since the minimum lumen F-actin intensity value indicates the extent of F-actin occluding the ring canal lumen. *P<0.05, ***P<0.0005, ****P<0.0001, One-way ANOVA test. Scale bar: (A) 1 μm.

Literature cited

Canning, P., C.D.O. Cooper, T. Krojer, J.W. Murray, A.C.W. Pike, A. Chaikuad, T. Keates, C. Thangaratnarajah, V. Hojzan, B.D. Marsden, O. Gileadi, S. Knapp, F. von Delft, and A.N. Bullock. 2013. Structural basis for Cul3 protein assembly with the BTB-Kelch family of E3 ubiquitin ligases. *J Biol Chem*. 288:7803–7814. doi:10.1074/jbc.M112.437996.

Deshaies, R.J. 1999. SCF and Cullin/Ring H2-based ubiquitin ligases. *Annu Rev Cell Dev Biol*. 15:435–467. doi:10.1146/annurev.cellbio.15.1.435.

Kelley, L.A., and M.J.E. Sternberg. 2009. Protein structure prediction on the Web: a case study using the Phyre server. *Nature protocols*. 4:363–371. doi:10.1038/nprot.2009.2.

Stogios, P.J., G.S. Downs, J.J.S. Jauhal, S.K. Nandra, and G.G. Privé. 2005. Sequence and structural analysis of BTB domain proteins. *Genome Biol*. 6:R82. doi:10.1186/gb-2005-6-10-r82.